Autocatalysis in the Conversion of Silica-supported $(CH_3)_2Au(acac)$ to Gold Nanoparticles

Taeho Hwang[1], Ryan C. Nelson[1], Miyako Hisamoto[1], Susannah L. Scott[1,2]*

[1] Department of Chemical Engineering, *University of California, Santa Barbara, CA 93106, U.S.A.*
[2] Department of Chemistry and Biochemistry, *University of California, Santa Barbara, CA 93106, U.S.A.*

23rd NAM Catalysis on the Fast Track — June 2-7, 2013 · Louisville, Kentucky · www.NAM23.org

Introduction

Gold nanoparticles (AuNPs) dispersed on oxide supports are highly active in a variety of oxidation reactions, including low-temperature CO oxidation [1]. Since their catalytic properties are a strong function of AuNP size and shape [2], the ability to control nanoparticle growth is key to catalyst optimization. The volatile organogold complex $(CH_3)_2Au(acac)$ (acac = acetylacetonate) has been well-studied in chemical vapor deposition (CVD). Once supported, it is readily transformed to gold nanoparticles by mild thermolysis or photolysis [3,4]. The initial binding of $(CH_3)_2Au(acac)$ to a dehydroxylated silica surface involves hydrogen bonding between surface silanols and the oxygen atoms of the acac ligand [5]. The goal of this study is to understand the kinetics and mechanism of the transformation to AuNPs, in order to identify key variables controlling particle nucleation and growth.

A series of thermal decompositions of $(CH_3)_2Au(acac)$ were conducted in various solvents and on a heterogeneous silica support. These studies were augmented with DFT calculations of various support and solvent models, which provided insight into the mechanism of this transformation.

$$(CH_3)_2Au(acac) / SiO_2 \xrightarrow{\blacktriangle} CH_3CH_3 + Au(0) / SiO_2 + Hacac / SiO_2$$

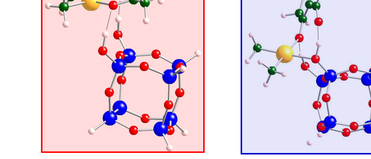

[1] Haruta, M. *Chem. Lett.* 16, 405 (1987).
[2] Haruta, M. *Chem. Rec.* 3, 75 (2003).
[3] Baum, T.H. *Organometallics* 8, 2477 (1989).
[4] Guzman, J. *J. Am. Chem. Soc.* 126, 2672 (2004).
[5] Hisamoto, M. *J. Phys. Chem. C.* 113, 8794 (2009).

Autocatalytic Evolution in Solution

A. Several isosbestic points are observed during the course of the reaction, indicative of a transformation without intermediate buildup. 304 nm $(CH_3)_2Au(acac)$; 272 nm acetylacetone (Hacac); 540-560 nm surface plasmon resonance of the AuNPs. The change in plasmon absorption maximum is due to increasing particle size. TEM image (a) shows large Au particles are produced (~100nm).

B. Kinetic profile extracted at three wavelengths from Fig (A), and curvefit using equation in Scheme 1 gives $k_1 = (2.207 \pm 0.364) \times 10^{-3}$ min^{-1} and $k_2 = (0.105 \pm 0.010)$ M^{-1}min^{-1}.

C. Acids increase the autocatalytic decomposition rate in dry CH_3CN as measured at 540 nm; the effect seems to be related to acid strength: water pK_a = 31.4; trifluoroethanol pK_a = 23.5. (pK_a values measured in dimethylsulfoxide)

D. With small additions of acids in dry benzene, an intermediate is detected during the decomposition.

(**A**) Typical UV-Vis spectra of a AuNP synthesis from $(CH_3)_2Au(acac)$ at 70 °C in iPrOH

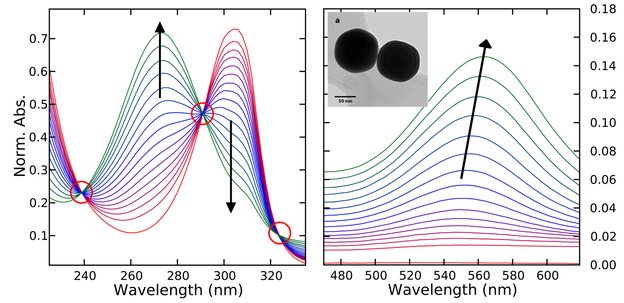

Scheme 1: Two step mechanism [6,7] and derived equation used to fit the kinetic data (Fig (B))

Nucleation

$$Au(III) \xrightarrow{k_1} Au(0)$$

Autocatalytic growth

$$Au(III) + Au(0)_n \xrightarrow{k_2} Au(0)_{n+1}$$

$$C_{A=Au(III)} = \frac{(k_1 + k_2 C_{A0}) C_{A0} e^{-(k_1 + k_2 C_{A0})t}}{k_1 + k_2 C_{A0} - k_2 C_{A0}(1 - e^{-(k_1 + k_2 C_{A0})t})}$$

[6] Watzky, M. *J. Am. Chem. Soc.* 119, 10382 (1997)
[7] Watzky, M. *J. Am. Chem. Soc.* 130, 11959 (2008)

(**B**) Three kinetic profiles in iPrOH and curvefits

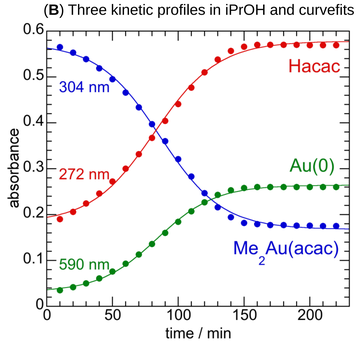

(**C**) In CH_3CN with various additives

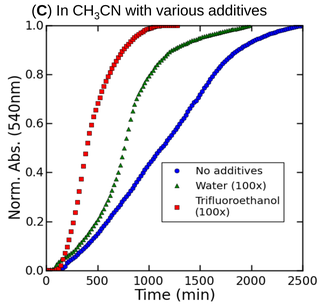

(**D**) In benzene with 1 eq. trifluoroethanol

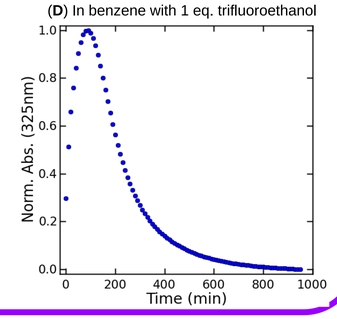

Double-autocatalytic Evolution on Silica

(**A**,**B**) IR spectra during the thermolysis of $(CH_3)_2Au(acac)/SiO_2$

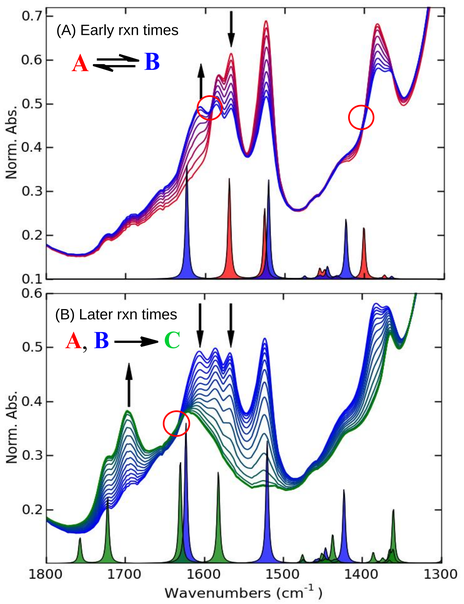

(**C**) Normalized kinetic profiles and their fits to Scheme 2.

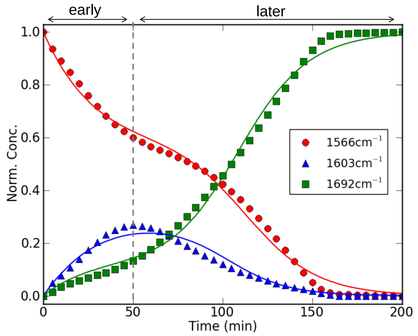

Scheme 2: The double-autocatalytic mechanism used to fit the kinetic data

$$A \underset{k_{-1}}{\overset{k_1}{\rightleftharpoons}} B$$

$$2A \xrightarrow{k_2} C$$

$$A + C \xrightarrow{k_3} 2C$$

$$B + C \xrightarrow{k_4} 2C$$

A. IR spectra taken during early reaction times of thermolysis of $(CH_3)_2Au(acac)$ supported on SiO_2 at 75 °C (the lines are the measured data). An isosbestic point at 1600 cm^{-1} suggests a clean transformation from starting material to the intermediate. The filled curves below the data are the DFT predicted spectra for the red(A)- and blue(B)-highlighted models in Fig D. (The predicted frequencies were scaled by 0.97 in order to highlight the overlap with the measured spectra.)

B. IR spectra of later reaction times. Again, a new isosbestic point is observed at 1630 cm^{-1}. The filled blue spectrum is for the same intermediate shown in Fig A; the filled green spectrum is a 1:1 combination of the predicted spectra of the keto and enol tautomers of Hacac, hydrogen-bonded to a silsesquioxane cube. (green(C)-highlighted models in Fig D).

C. Three distinct kinetic profiles were extracted from in situ IR spectra in Figures A and B (shown as the solid points). Absorbance at 1566cm^{-1} and 1603cm^{-1} are normalized. This unusual kinetic profile was fit to the double-autocatalytic decomposition mechanism shown in Scheme 2 (shown as lines). This is the minimal kinetic model necessary to fit this data.

D. DFT structures of silica supported reaction complexes. Red-, blue- and green-highlighted models show the structures of A, B and C of Scheme 1, respectively.

Controlling relative rates of nucleation / growth

1. Reaction temperature

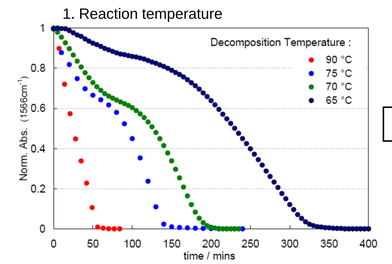

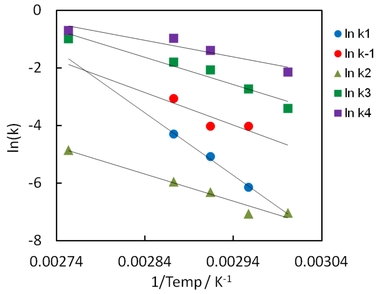

2. Surface OH content

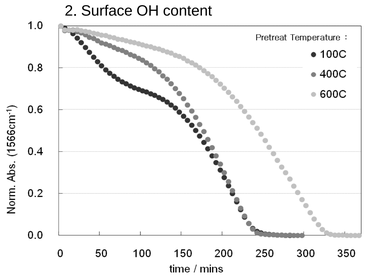

3. Au loading (A380_100ºC, 70ºC decomposition)

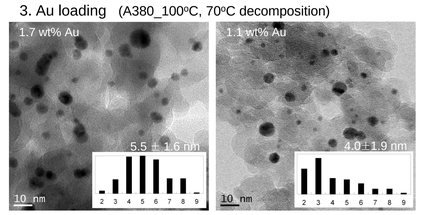

(**D**) Three silica-supported Au structures from DFT simulation. Each structure gives predicted IR spectra, shown in Fig A, B

DFT Functional = B3LYP
Basis Sets: Au = Mod. Lanl2DZ
Other atoms = 6-31Gd'

Conclusions

In situ IR spectroscopy is an ideal tool to monitor the thermal conversion of silica-supported $(CH_3)_2Au(acac)$ to AuNPs, because of the strong and distinctive spectra of the acac ligand (reactant) and Hacac (product). The resulting absorbance-time profiles are clearly autocatalytic, but they also show evidence for an intermediate whose concentration reaches a maximum at ca. 50 min. Based on comparison to the predicted vibrational spectra of DFT cluster models, we propose that this intermediate is the product of reversible silanol insertion into the Au(acac) chelate ring. A kinetic model was constructed with autocatalysis by Au(0), shown in solution phase kinetics. The resulting equations generate reasonable curve-fits. The organogold loading, silanol density and reaction temperature affect the relative rates of nanoparticle nucleation (spontaneous formation of Au(0) from $(CH_3)_2Au(acac)$ and the intermediate) and growth (autocatalytic decomposition of $(CH_3)_2Au(acac)$ and the intermediate, promoted by Au(0)). These parameters in turn affect the average nanoparticle size and size distribution, allowing us to optimize particle formation conditions for the desired diameter.

Acknowledgement Financial support of the US DOE under the Catalysis Science Initiative (DE-FG-02-03ER15467)